Article

Evaluating the Relation of Cave Passage Formation to Stress-Field: Spatio-Temporal Correlation of Speleogenesis with Active Tectonics in Asprorema Cave (Mt. Pinovo, Greece)

Georgios Lazaridis [1], Emmanouil Katrivanos [1], Despoina Dora [1], Lambrini Papadopoulou [1], Ilias Lazos [2,*] and Alexandros Chatzipetros [1]

1   School of Geology, Aristotle University of Thessaloniki, 54124 Thessaloniki, Greece; geolaz@geo.auth.gr (G.L.); ekatriva@geo.auth.gr (E.K.); despdora@geo.auth.gr (D.D.); lambrini@geo.auth.gr (L.P.); ac@geo.auth.gr (A.C.)
2   School of Mineral Resources Engineering, Technical University of Crete, 73100 Chania, Greece
*   Correspondence: ilazos@tuc.gr

Abstract: Caves serve as time capsules, preserving significant markers of tectonic activity and offering insights into geological history. Fault geometries and past activations found in caves can be correlated with known deformational events in the broader area, temporally delimiting the speleogenesis. More specifically, cave passage formation is suggested to be affected by the regional stress-field. The Asprorema Cave in Northern Greece is a typical example of a fracture guided cave, with passage geometry influenced by relative sidewall movements, revealing these discontinuities as faults. This study constructs the timeframe and conceptual model of speleogenesis in relation to tectonic events, geomorphological evolution and hydrological zones, and verifies its relation to the stress-field. Active tectonics, mineralogy and cave geomorphology are investigated. Results suggest syntectonic speleogenesis under phreatic and epiphreatic conditions. The absence of corrosion on fault slip surfaces implies recent activations post cave's shift to the vadose zone. Structural analysis identifies three main neotectonic phases: NNW-SSE striking faults (oldest group of structures), NE-SW striking faults with dextral strike-slip movement (post-middle Miocene), and NE-SW striking normal faults indicating extensional stress-regime (Quartenary). The last two phases affect cave passage shape causing wall displacement, highlighting passage formation along discontinuities perpendicular to the horizontal minimum stress axis.

Keywords: cavitonics; neotectonics; fault; structural analysis; conceptual speleogenesis model

1. Introduction

Caves preserve evidence of geological processes that have acted and formed the landscape. Researchers often turn to speleological research for reconstructing paleoenvironment, paleoclimate [1], and paleohydrology [2], providing insights into the geological history of an area. Over the last decades, caves have evolved into natural laboratories of neotectonics. Neotectonics are conserved in some cave systems (e.g., [3]), dependent on different factors, such as time, cave climate, the deformation of features, etc. Studying features related to neotectonic activity and their deformation dating has led to dating earthquakes [4,5], comparing underground and the surface microdisplacement of a tectonic fault [6], proving active tectonics in intracratonic settings [7], and investigating the relation between the pattern of cave passages and the neotectonic stress field [8].

Asprorema Cave is among the few caves systematically investigated for active tectonic evidence in Greece, along with Korakia Cave in Pserimos Island in the Dodecanese [9]. Tectonic data obtained from the cave's interior are correlated with the areal stress field and the passage pattern of the Asprorema Cave, enabling the detection of preferred direction development. Features formed from tectonic activity in the Asprorema Cave provide data for building the timeline of speleogenetic and tectonic events.

Among various possible indicators of tectonic activity in caves are broken speleothems, growth anomalies in speleothems, ceiling breakdown, bedding plane slip, deformation in cave sediment structures and fault displacements (e.g., [5,10,11]). Displacements in the passage profile stand as an unquestionable proof of tectonic activity [4,12]. The analysis of speleothem deformation has been broadly used for dating and evaluating paleoseismic and tectonic events [13–16].

Identification of the deformation mechanism is a key point of researching tectonic activity, or "cavitonics" [8], in caves. In general, caves experience lower levels of erosion compared to the surface geomorphological features favoring such identifications. On the other hand, various non-tectonic processes factors, such as human activity, gravity and mechanical failure of the host rock known as ceiling breakdown, snow accumulation and freezing phenomena, etc., can displace or deform cave features.

This study aims to evaluate the hypothesis that cave passages are formed along discontinuities that have a perpendicular orientation to the horizontal minimum stress axis (see [8,17]) based on detailed study of tectonic, depositional and geomorphic features in the Asprorema Cave: a small cave where multiple fault planes of specific geometry are found to deform passage shape, whereas tectonic discontinuities with different orientation do not display post-speleogenetic affection to passage shape. Furthermore, there are antithetical faults and well-preserved slicken lines on the fault planes. In total, these features make this cave a suitable example to evaluate the above-mentioned hypothesis.

2. Geological Setting—Deformation History

Asprorema Cave, also known as Gardanska according to testimonies of the locals, is located in Mt. Pinovo in Northern Greece, at an altitude of 620 m above sea level (asl), within the valley that is shaped from the Asprorema stream (Figure 1). The cave entrance is overhanging on the steep limestone slope with a NE orientation. Along the Pinovon/Tzena Mts. front, Holocene-age alluvial fans have been deposited extensively, while travertine deposits have also developed significantly (1:50,000 geological maps of IGME, Promahi and Skra sheets; [18,19]). The Upper Cretaceous limestone where Asprorema Cave is formed, overlies the Upper Jurassic alterations of crystalline limestone and green schist which are part of the spillites—keratophyres series. All the sequence represents the overthrust of the Mt. Pinovo nappe [20,21].

The Pinovon/Tzena and Paikon tectonostratigraphic terranes are located in the central part of the Axios zone, between the Almopia ophiolitic belt to the west and the Paionia ophiolitic belt to the east [22–31].

According to the newest tectonostratigraphic data [20,21,32], these terranes consist of similar tectonostratigraphic units. They constitute a single tectonic nappe pile that has undergone the same polyphase deformation and metamorphism (D1–D6) from the Mid-Jurassic to recent times. The shortening alternated with the extension, while the deformation conditions evolved from ductile (D1 to D3, Jurassic until Cretaceous) to brittle (D4 to D6, Tertiary to the present). Compressional events are linked to ophiolite obduction, nappe stacking, crustal thickening and terrane accretion, while extensional events are associated with orogenic collapse, crustal thinning, terrane dispersion and basin formation [20]. Upper Cretaceous extension (D3 event) and the exhumation of deeper crustal rocks are associated with basin subsidence and deposition of the Upper Cretaceous limestones and flysch (Cenomanian to Maestrichtian), which outcrops on the western flanks of the Paikon and Pinovon Mts [20]. This single tectonic nappe pile eventually evolved into multiple tectonic windows due to successive compressional and extensional events from the Jurassic to the Tertiary. The final exhumation of Pinovon/Tzena and Paikon tectonostratigraphic units occurred during the Oligocene–Miocene extensional event in brittle conditions (D5).
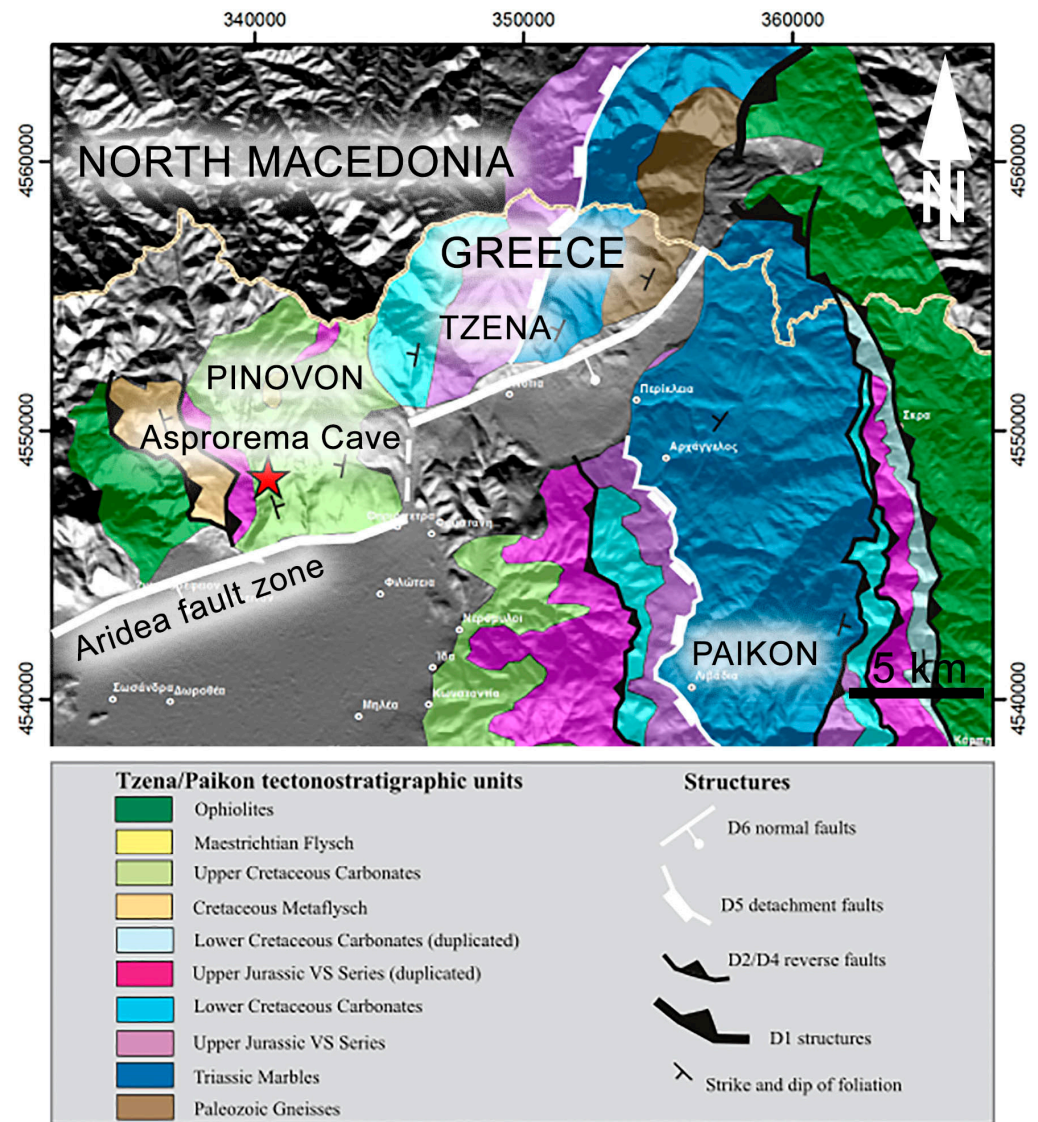
Figure 1. Geological map of the Pinovon-Tzena and Paiko terranes, depicting the main deformational events and the location of Asprorema Cave indicated with red star (projection GGRS87; modified map from [20,21]).

During the Miocene–Pliocene, the D6 extensional event caused faulting, overprinting all the previously formed structures. D6 structures include high-angle normal, dip-slip to oblique faults, as well as strike-slip faults [32]. A crucial D6 fault is the ENE-WSW striking and SSE dipping Aridea fault zone, originally considered a dextral strike-slip fault, reactivated during the Pliocene–Quaternary until recently as a normal dip-slip fault [20,33]. The activity of this fault has separated the Pinovon/Tzena from the Paikon terrane, forming the Neogene to Quaternary "Notia" depression and leading to post-accretional terrane dispersion [20,21,32,34].

3. Methods

During field work the cave has been observed exhaustively for geomorphological indicators of speleogenesis, known as speleogens, along with speleothem identification and structural analysis. In addition, the cave was surveyed to a grade 5 map [35] according to standard cave techniques (i.e., [36,37]) and scanned with a LIDAR sensor built in iPhone13 pro and the application Polycam. Rock discontinuities were measured using a Clar compass in areas unaffected by breakdown. Tectonic activity was identified by passage shape displacements. Measurements include fault planes, slicken lines with kinematic indicators,

superposition of striae, dip, and strike. Terminology for dissolutional forms, used to identify the conditions of speleogenesis can be found in the suggested literature [38–41].

Scallops (see [42–45]) were systematically surveyed within various locations along the deepest cave passage. The amassed dataset was subjected to rigorous analysis using the specialized spreadsheet program "Scallopex", following the methodology outlined by Woodward and Sasowsky [46]. Specific parameters, including scallop lengths, water temperature, and passage diameter and shape, were input into the software. Scallop lengths were measured in centimeters to one decimal point of accuracy, assuming a constant water temperature of 5 °C. This choice of temperature approximates the lowermost recorded water temperatures within the regional cave systems, even during the colder climate periods and consequently facilitated estimations of water velocity closely approximating the cave's maximum attainable flow rates. Subsequently, the results underwent thorough statistical analysis using the "PAST 3.2" statistical software, following the methodology articulated by Hammer et al. [47].

GeoRose 0.5.1. software was utilized to process passage orientations from the most detailed map of the cave created from the 3d scan. Similarly, rose diagrams from the hydrothermal caves of the broader area were drawn for comparison, following the method outlined by Littva et al. [8].

The geomorphological data were interpreted in terms of speleogenetic events, while the tectonic data were utilized to identify fault activations in various stress fields. These findings were correlated with the known deformation events in the broader area and with speleogenesis, providing a timeframe for distinct phases.

Morphological and chemical investigations of a white-colored floor deposit sample was carried out in the Scanning Microscope Laboratory of Aristotle University of Thessaloniki (A.U.Th.), using a JEOL JSM6390LV Scanning Electron Microscope (SEM) equipped with an Energy Dispersive Spectrometer (EDS) INCA 250, with 20 kV accelerating voltage and 0.4 mA probe current. Pure cobalt (Co) was used as an optimization element.

4. Results

4.1. Cave Geomorphology

The entrance to the Asprorema cave is situated along a fault escarpment, approximately 30 m above the adjacent riverbed (Figure 2; for a 3d scan: https://speleology8.wordpress.com/asprorema-cave/, accessed on 11 March 2024). The vertical extent of the cave, from the highest to lowest point, measures approximately 17 m. The plan length of the cave is 33 m. The deepest recesses of the cave are obscured by accumulations of clastic sediments, although the morphology of the passages suggests a further descent.

The cave primarily comprises a principal narrow, high corridor, characterized by a prevailing east–west to northeast–southwest orientation, featuring a gently sloping floor. Several narrower passages, oriented in a northwest-southeast direction, intersect transversely with the primary corridor. Towards the southeast section of the cave, the main corridor shifts direction, leading to a smaller passage with a parallel orientation, leading to an intermediate inclined chamber with a wide layout and a low ceiling.

The mesoscale morphology of the cave passages appears elliptical, when viewed in cross-section, with the long axis transitioning from predominantly vertical near the cave entrance, to more horizontal orientation at deeper levels. This phenomenon is a result of the influence of structural rock discontinuities, given that the passages are guided by fractures. Small-scale dissolution features, primarily associated with cupolas, are notable.

Cupolas exhibit a fracture-guided pattern and occasionally form configurations resembling rock bridges. Relics of wall rock material resulting from the intersection of cupolas, known as cusps, have been identified within the cave. These cupolas manifest a complex upward branching structure, often giving rise to the formation of cupolas within other cupolas. Moreover, scallops, serving as discernible small-scale geomorphic features, are abundant within the inner recesses of the cave, including on the cave ceiling within the inclined northwest-southeast passage. By analyzing the presence and distribution of these

scallops, a noteworthy maximum flow rate of 0.65 m/s directed towards the southeast has been estimated.
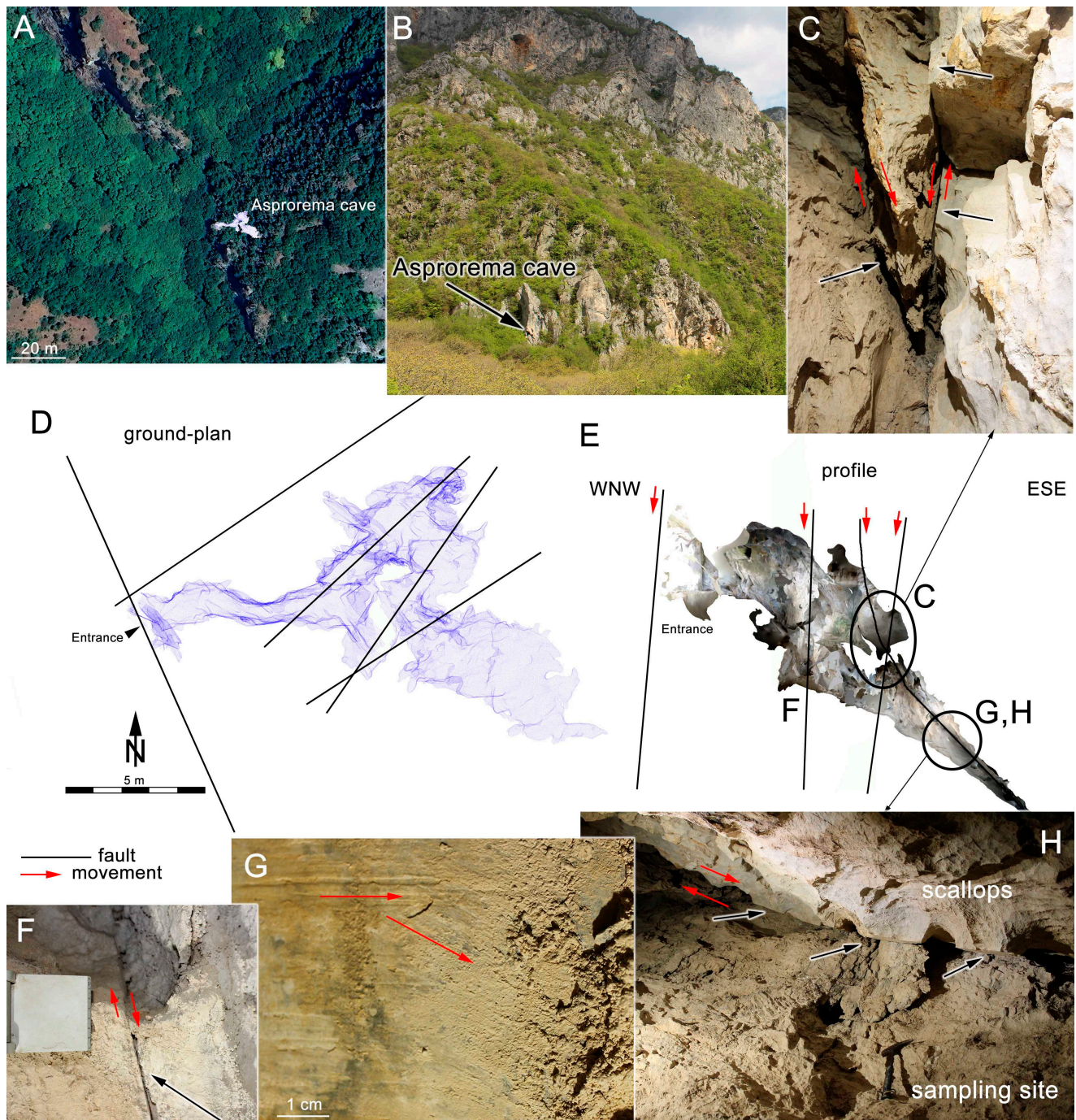
Figure 2. Asprorema Cave: (**A**). Aerial view (Google Earth) of the location with the cave ground plan projected. (**B**). Entrance location. (**C**). Conjugated faults. (**D**). Ground plan. (**E**). Profile. (**F**). Displaced passage shape. (**G**). Slicken lines of two distinct tectonic events on a fault plane. (**H**). Displaced passage along a medium dip-angle fault plane, with displaced karst tubes. Red arrows indicate fault movement and black arrows indicate fault planes.

4.2. Mineralogy

A distinct, white-colored fragile layer is disclosed in the floor clastic sediments of the innermost part of the cave (Figure 2H). EDS-SEM analyses of this material indicate the presence of various elements, primarily Ca, Si, and S. The elements Al, Mg, K, Na,

Fe, and Ti are incorporated into morphologically platy minerals, likely corresponding to aluminosilicates (Figure 3A). Needle-like and spherical forms with high Si and Ca content are interpreted as silicate and carbonate minerals (Figure 3B). These can be amorphous SiO_2, and calcite and aragonite, respectively. Some crystallites smaller than 10 μm, form aggregates that contain S and Ca, suggesting the presence of gypsum (Figure 3C). Apart from the aluminosilicates, a secondary origin is suggested for the other minerals.
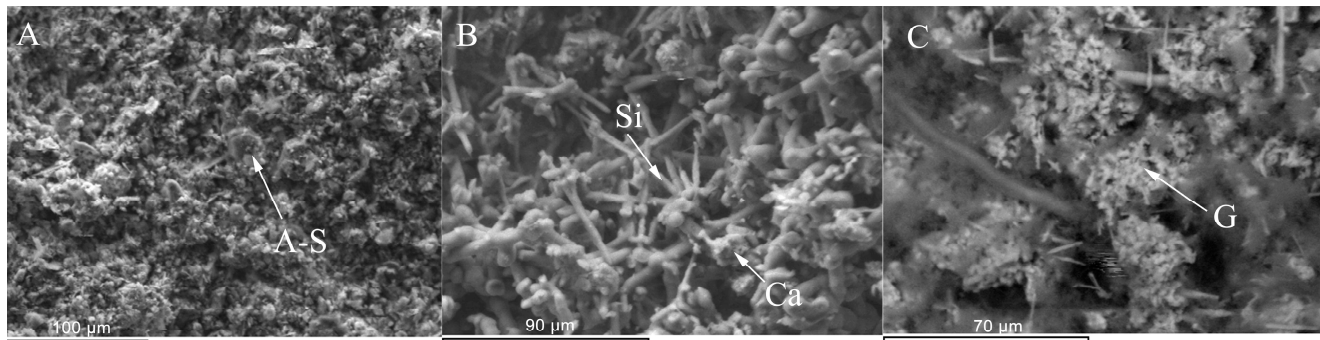
Figure 3. Scanning electron microscopy images of the layer collected from the Asprorema Cave. (**A**). Platy aluminosilicate (A-S) minerals. (**B**). Needle-like and spherical aggregates of silicates (Si) and carbonates (Ca). (**C**). Gypsum aggregates.

Apart from this layer, all other authigenic secondary minerals are mainly calcite speleothems such as stalactites, flowstone and coraloids.

4.3. Cave Tectonics

A faulty plane with NNW-SSE orientation defines the escarpment at the cave entrance, exhibiting striations on its plane. However, it is worth noticing that this fault, along with any parallel tectonic discontinuities within the cave interior, shows no evidence of passage shape deformation or recent activity.

In contrast to this fault plane, certain surfaces on both the sidewalls and the ceiling exhibit no discernible dissolution features but instead display slicken lines. Furthermore, these slicken-lined surfaces are conductive in reshaping the passages, providing clear evidence of relative movement and translocation of the sidewalls. These surfaces correspond to a fault plane with a NE-SW strike and an intermediate dip angle in the innermost cave passage, dipping towards the SW. Additionally, there are a few antithetic high dip-angle faults influencing the formation of the remaining passages.

The D6 deformation phase has been described in general by Pavlides et al. [33] and Katrivanos et al. [20,32]. Detailed structural analysis of conjugated faults and striations in the cave reveals three main neotectonic phases (Figure 4). The first phase (D6a) is characterized by faults-oriented NNW-SSE, exhibiting dextral strike-slip movement. The second phase (D6b) involves NE-SW striking faults with dextral strike-slip movement. The youngest phase (D6c) consists of normal faults with NE-SW strike, indicating an extensional stress regime. The σ1 stress-axis is nearly vertical, with σ3 sub-horizontal, indicating NW-SE extension.
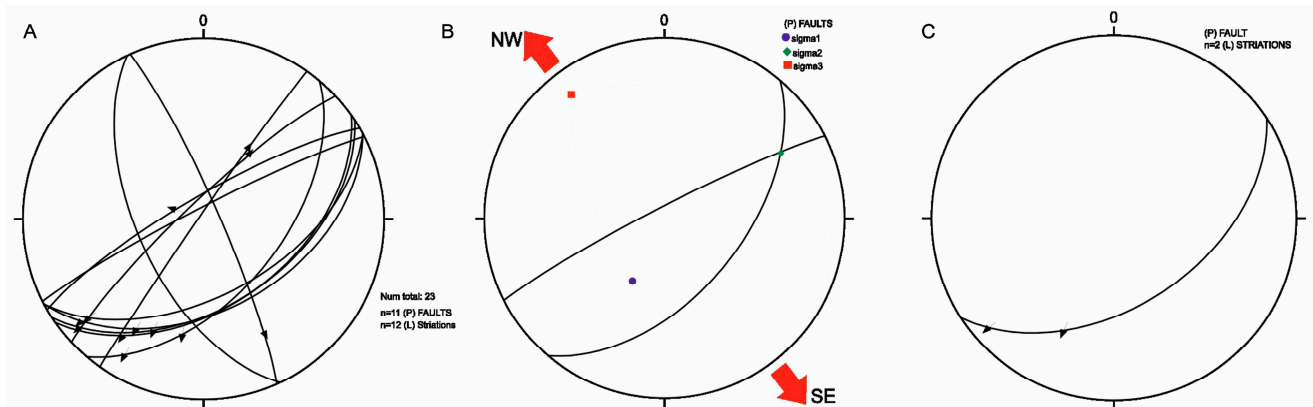
Figure 4. Schmidt diagrams of Asprorema Cave with: (**A**). all faults and striations measured; (**B**). conjugated faults; and (**C**). two striations on a particular fault plane.

5. Discussion

The morphology of the Asprorema Cave is indicative of a phreatic speleogenesis (e.g., [48]), which means its passages were shaped while fully submerged in the aquifer. This stage formed the mesoscale morphology of the passages with elliptical cross-sections and the cupola-related morphology. The relatively high velocity indicated by the scallops (Figure 2H) along with the inward direction of flow, suggests that while in the epiphreatic zone the cave was flooded by the Asprorema stream. These events occurred before the 30 m downcutting from the cave entrance level to the recent riverbed. The phase of turbulent water flow and scallop formation was followed by fine-grained clastic sedimentation and the formation of the layer with the authigenic fragile needle-like silicates and gypsum that would have been easily removed under intense flow. These sediments mark a distinct phase of low energy water flow to stagnant water in the cave.

Karst dissolution forms cave passages along discontinuities that have a perpendicular orientation to the horizontal minimum stress axis (see [8,17]). While this assumption has not been tested in every geotectonic regime, it appears valid for the Asprorema cave. Our case study provides evidence of neotectonic structures deforming cave passages (Figure 2F–H and 3D model) and links their orientation with neotectonic activity (Figure 4). Therefore, it is reasonable to assume that these deformed fault-guided passages were initially formed in the same regime by a syntectonic process of speleogenesis. Later, these passages were deformed by fault re-activations.

Furthermore, we compared the rose diagram pattern of the passage orientation in Asprorema Cave with those from the caves of the Almopia Speleopark (Figure 5), located in proximity to Asprorema Cave and formed by hydrothermal hypogene speleogenesis [49–51]. Asprorema Cave displays a major passage with a NE-SW orientation and a minor one striking ESE-WNW. Among the Almopia caves, Varathro cave, the largest one, also displays a NE-SW major passage orientation and an ENE-WSW secondary one, parallel to the large neotectonic Aridea fault [20,32]. However, the total Almopia Speleopark passage orientation is NW-SE and ENE-WSW. In addition, no active faults and deformed passages have been observed throughout careful investigation of all the Almopia Speleopark caves (e.g., [50] and this study), indicating that the Asprorema cave is a unique case for the area.

The Asprorema Cave has been formed along discontinuities, which define three main neotectonic phases that are in agreement with previous neotectonic studies in the broader region. These studies consider the deformation phase (D6) to be of late Miocene to Quaternary age [33].We suggest a timeframe and a conceptual model of speleogenesis in relation to tectonic events (D6a-c, as identified in this study), geomorphological evolution, and hydrological zones (Figure 6). Initiation of speleogenesis postdates the early geotectonic regime that led to the formation of the NNW-SSE dextral strike-slip faults of phase D6a during the Late Miocene. While these structures define the Asprorema Stream, they do not deform the morphology of cave passages. The predominant orientation of cave passages

along NE-SW orientation (Figure 2D,E and Figure 5) is indicative of dissolution in a regime of NW-SE extension. During this phase, passages are formed along the faults of the D6b phase, with an orientation perpendicular to the horizontal minimum stress axis. This extensional phase is related to the uplift, resulting in a drop in the water table and the shift of the cave from the phreatic to the epiphreatic hydrological zone (Figure 6). Under flooding conditions in this zone, scallops have been formed.
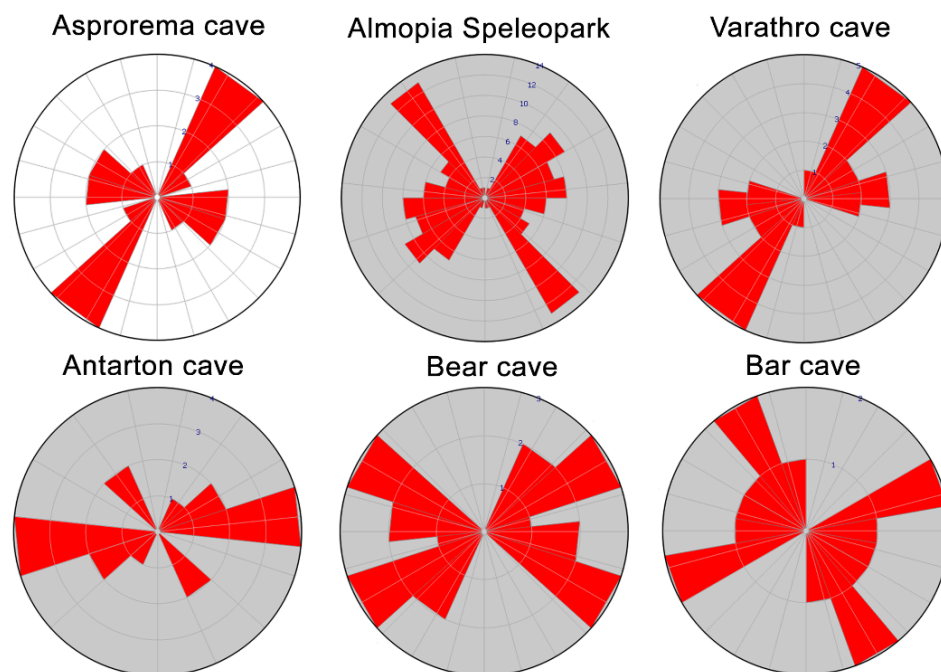
Figure 5. Comparison of rose-diagram with Asprorema cave passages and other documented caves of the area formed by hydrothermal hypogene speleogenesis. Passage orientations for the Almopia Speleopark caves are taken from cave ground-plans in Lazaridis, 2006. The count of passages varies among the examined caves and subsequently the n of orientations plotted on the rose-diagrams.

Downcutting isolated the cave from surficial stream recharge, and this allowed any slickensides that formed by tectonic activity of the fault-guided passages to remain intact by dissolution. Fragile needle-like silicates and gypsum formed under stagnant water conditions during this stage of cave development.

In general, and up to our knowledge, speleological studies have not identified small-scale (smaller than passage dimensions) morphological features that are indicative of syntectonic passage development. Our field observations and comprehensive examinations of the three-dimensional cave model constructed have signified the absence of morphological indicators related to syntectonic development. Essentially, our findings indicate that, apart from the most recent deformations enduring dissolution within the vadose conditions of the cave environment, there are no discernible indicators correlating the timeframe of speleogenesis with the corresponding stress-field. Consequently, deformations in passage shape resulting from fault activations during syntectonic speleogenesis are likely to manifest as small-scale morphological features, which are easily obliterated by dissolution processes. In contrast, the cave pattern is the morhological element, which is difficult to get modified by events subsequent to the speleogenesis. Hence, many fault-guided cave passages may have undergone syntectonic development and lack discernible markers if faults remain inactive or have not reactivated after cave shifting from the phreatic to the vadose zone.
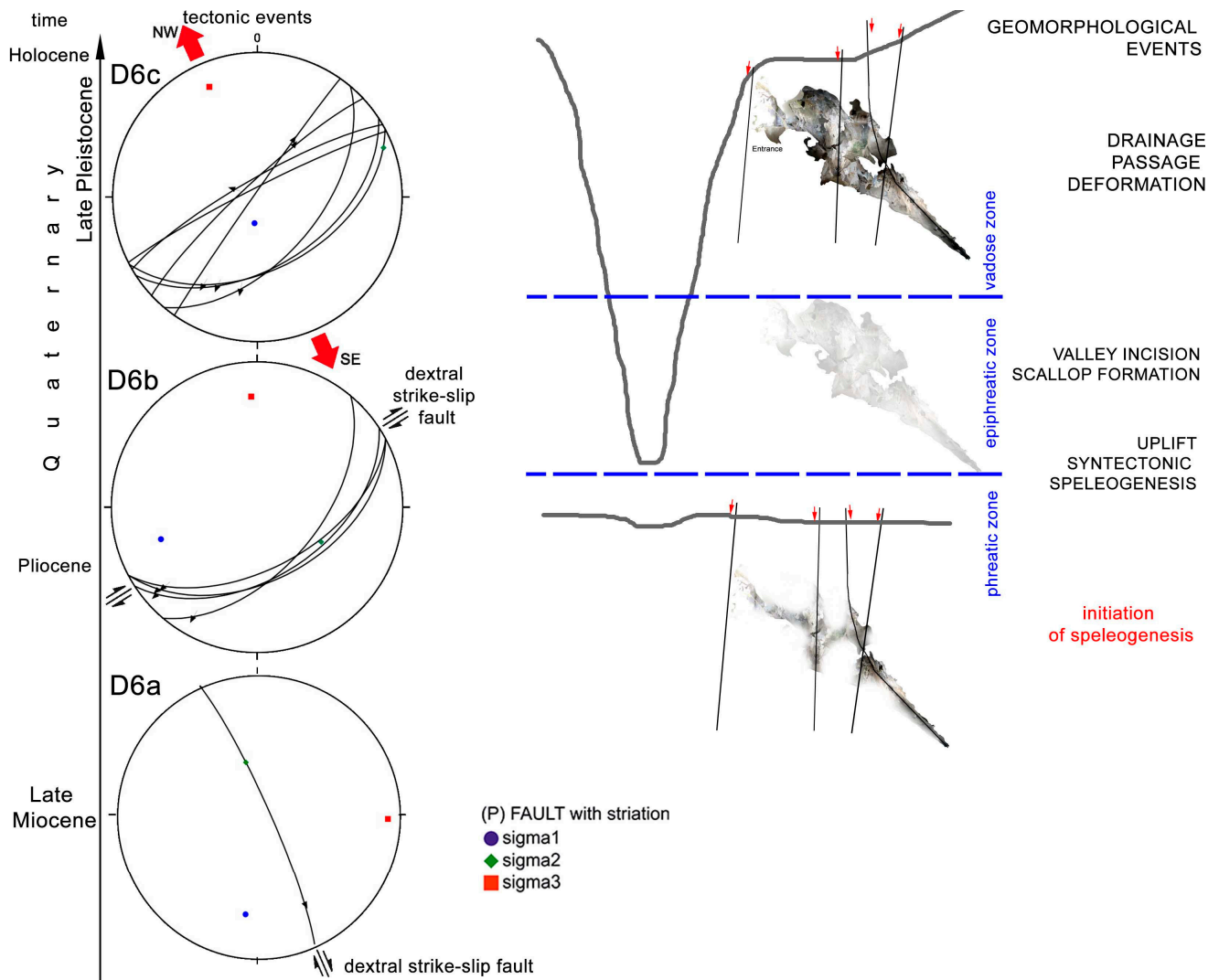
Figure 6. Timeframe and conceptual model of speleogenesis in relation to tectonic events, geomorphological evolution, and hydrological zones. Arrows indicate fault movement except of D6c where arrows indicate the orientation of the extension.

6. Conclusions

The study of Asprorema Cave highlights the hypothesis that cave passages are formed along discontinuities of perpendicular orientation to the horizontal minimum stress axis. Geomorphological and structural analysis of the cave passages verify that speleogenesis is guided by the stress field of the area.

Three deformation phases (D6a-c) of post-Middle Miocene to Late Pleistocene age have been identified. The faults of phases D6b and D6c deform the cave passages, whereas D6a does not display any signs of reactivations affecting the cave morphology. This study strengthens the significance of caves in preserving tectonic history that may be difficult to observe on the surface.

Author Contributions: Conceptualization, G.L.; methodology, G.L., E.K. and D.D.; field-work, G.L., E.K. and D.D.; data analysis, all authors; laboratory analysis: L.P.; writing—original draft preparation, G.L. with input from all authors. All authors have read and agreed to the published version of the manuscript.

References

1. White, W.B. Cave sediments and paleoclimate. *J. Cave Karst Stud.* **2007**, *69*, 76–93.
2. Frumkin, A.; Fischhendler, I. Morphometry and distribution of isolated caves as a guide for phreatic and confined paleohydrological conditions. *Geomorphology* **2005**, *67*, 457–471. [CrossRef]
3. Baroň, I.; Plan, L.; Sokol, L.; Grasemann, B.; Melichar, R.; Mitrovic, I.; Stemberk, J. Present-day kinematic behaviour of active faults in the Eastern Alps. *Tectonophysics* **2019**, *752*, 1–23. [CrossRef]
4. Becker:, A.; Davenport, C.A.; Eichenberger, U.; Gilli, E.; Jeannin, P.Y.; Lacave, C. Speleoseismology: A critical perspective. *J. Seismol.* **2006**, *10*, 371–388. [CrossRef]
5. Becker, A.; Häuselmann, P.; Eikenberg, J.; Gilli, E. Active tectonics and earthquake destructions in caves of northern and central Switzerland. *Int. J. Speleol.* **2012**, *41*, 5. [CrossRef]
6. Briestenský, M.; Košťák, B.; Stemberk, J.; Petro, L.; Vozar, J.; Fojtikova, L. Active tectonic fault microdisplacement analyses: A comparison of results from surface and underground monitoring in western Slovakia. *Acta Geodyn. Geomater.* **2010**, *7*, 387–397.
7. Briestenský, M.; Stemberk, J.; Michalik, J.; Bella, P.; Rowberry, M. The use of a karstic cave system in a study of active tectonics: Fault movements recorded at driny cave, male Karpaty mts (Slovakia). *J. Cave Karst Stud.* **2011**, *73*, 114–123. [CrossRef]
8. Littva, J.; Hok, J.; Bella, P. Cavitonics: Using caves in active tectonic studies (Western Carpathians, case study). *J. Struct. Geol.* **2015**, *80*, 47–56. [CrossRef]
9. Grasemann, B.; Plan, L.; Baroň, I.; Scholz, D. Co-seismic deformation of the 2017 Mw 6.6 Bodrum–Kos earthquake in speleothems of Korakia Cave (Pserimos, Dodecanese, Greece). *Geomorphology* **2022**, *402*, 108137. [CrossRef]
10. Postpischl, D.; Agostini, S.; Forti, P.; Quinif, Y. Palaeoseismicity from karst sediments: The »Grotta del Cervo« cave case study (central Italy). In *Investigation of Historical Earthquakes in Europe*; Stucchi, M., Postpischl, D., Slejko, D., Eds.; Tectonophysics: Amsterdam, The Netherlands, 1991; Volume 193, pp. 33–44.
11. Šebela, S. Broken speleothems as indicators of tectonic movements. *Acta Carsologica* **2008**, *37*, 51–62. [CrossRef]
12. Szczygieł, J. Quaternary faulting in the Tatra Mountains, evidence from cave morphology and fault-slip analysis. *Geol. Carpathica* **2015**, *66*, 245–254. [CrossRef]
13. Forti, P.; Postpischl, D. Seismotectonic and paleoseismic analyses using karst sediments. *Mar. Geol.* **1984**, *55*, 145–161. [CrossRef]
14. Delaby, S. Palaeoseismic investigations in Belgian caves. *Geol. En Mijnb.* **2001**, *80*, 323–332. [CrossRef]
15. Gilli, É. Review on the use of natural cave speleothems as palaeoseismic or neotectonics indicators. *Comptes Rendus Geosci.* **2005**, *337*, 1208–1215. [CrossRef]
16. Kagan, E.J.; Agnon, A.; Bar-Matthews, M.; Ayalon, A. Dating large infrequent earthquakes by damaged cave deposits. *Geology* **2005**, *33*, 261–264. [CrossRef]
17. Shanov, S.; Kostov, K. *Dynamic Tectonics and Karst*; Springer: Berlin/Heidelberg, Germany, 2014.
18. Mavrides, A.; Matarangas, D.; Karfakis, J. *Geological Map of Greece, 1:50000, Skra Sheet*; Institute of Geology and Mineral Exploration: Athens, Greece, 1982.
19. Galeos, A.; Karfakis, J.; Photiades, A. *Geological Map of Greece, 1:50000, Promahi Sheet*; Institute of Geology and Mineral Exploration: Athens, Greece, 2003.
20. Katrivanos, E.; Kilias, A.; Mountrakis, D. Deformation history and correlation of Paikon and Tzena Terranes (Axios zone, Central Macedonia, Greece). *Bull. Geol. Soc. Greece* **2016**, *50*, 34–45. [CrossRef]
21. Katrivanos, E. Structure, Kinematics and Tectonics of Paikon and Tzena Mountains (Central Macedonia, Greece). Ph.D. Thesis, Aristotle University, Department of Geology, Thessaloniki, Greece, 2017; p. 244.
22. Mercier, J. Etude geologique des zones Internes des Hellenides en Macedoine centralle. Contribution a l' etude du metamorphisme et de l' evolution magmatique des zones internes des Hellenides. *Ann. Geol. Pays Hell.* **1968**, *20*, 1–739.
23. Godfriaux, I.; Ricou, L.E. Le Paicon, une fenetre tectonique dans les Hellenides Internes (Macedoine, Grece). *C. R. Acad. Sci. Paris* **1991**, *313*, 1479–1484.
24. Ricou, L.E.; Godfriaux, I. Une coupe a travers les ophiolites et gneiss allocthones entre le massif Pelagonien et la fenetre du Paikon (Grece du Nord). *C. R. Acad. Sci. Paris* **1991**, *313*, 1595–1601.
25. Ricou, L.E.; Godfriaux, I. Mise au point sur la fenetre multiple du Paicon et la structure du Vardar en Grece. *C. R. Acad. Sci. Paris* **1995**, *321*, 601–608.
26. Bonneau, M.; Godfriaux, I.; Moulas, Y.; Fourcade, E.; Masse, J. Stratigraphie et structure de la bordure orientale de la double fenetre du Paikon (Macedoine, Grece). *Bull. Geol. Soc. Greece* **1994**, *30*, 105–114.

27. Brown, S.; Robertson, A. New structural evidence from the Mesozoic-early Tertiary Paicon unit, Northern Greece. *Bull. Geol. Soc. Greece* **1994**, *30*, 159–170.

28. Brown, S.; Robertson, A. Sedimentary geology as a key to understanding the tectonic evolution of the Mesozoic—Early Tertiary Paikon Massif, Vardar suture zone, N. Greece. *Sediment. Geol.* **2003**, *160*, 179–212. [CrossRef]

29. Ferriere, J.; Bonneau, M.; Caridroit, M.; Bellier, J.P.; Gorican, S.; Kollmann, H. Les nappes tertiaires du Paikon (zone de Vardar, Macédoine, Grèce): Arguments stratigraphique pour une nouvelle interprétation structurale. *Comptes Rendus L'académie Sci.-Ser. IIA-Earth Planet. Sci.* **2001**, *332*, 695–702.

30. Mercier, J.; Vergely, P. The Paikon Massif revisited comments on the Late Cretaceous—Paleogene geodynamics of the Axios-Vardar zone. How many Jurassic ophiolitic basins? (Hellenides, Macedonia, Greece). *Bull. Geol. Soc. Greece* **2001**, *34*, 2099–2112. [CrossRef]

31. Papanikolaou, D. Tectonostratigraphic models of the Alpine terranes and subduction history of the Hellenides. *Tectonophysics* **2013**, *595–596*, 1–24. [CrossRef]

32. Katrivanos, E.; Kilias, A. and Mountrakis, D. Kinematics of deformation and structural evolution of the Paikon Massif (Central Macedonia, Greece): A Pelagonian tectonic window? *N. Jb. Geol. Palaeont. Abh.* **2013**, *269*, 149–171. [CrossRef]

33. Pavlides, S.; Mountrakis, D.; Kilias, A.; Tranos, M. The role of strikeslip movements in the extensional area of the northern Aegean (Greece). *Ann. Tecton.* **1990**, *4*, 196–211.

34. Katrivanos, E.; Mountrakis, D.; Kilias, A.; Pavlides, S. Preliminary results of the geological structure and kinematics of deformation in Tzena Mt. (Paikon Subzone, Central Macedonia, Greece). *Bull. Geol. Soc. Greece* **2001**, *34*, 137–147. (In Greek) [CrossRef]

35. Häuselmann, P. UIS mapping grades. *Int. J. Speleol.* **2011**, *40*, 15.

36. Dasher, G.R. *On Station: A Complete Handbook for Surveying and Mapping Caves*; National Speleological Society: Huntsville, AL, USA, 1994.

37. Trimmis, K.P. Paperless mapping and cave archaeology: A review on the application of DistoX survey method in archaeological cave sites. *J. Archaeol. Sci. Rep.* **2018**, *18*, 399–407. [CrossRef]

38. Lauritzen, S.-E.; Lundberg, J. Solutional and erosional morphology of caves. In *Speleogenesis. Evolution of Karst Aquifers*; Klimchouk, A., Ford, D.C., Palmer, A.N., Dreybrodt, W., Eds.; National Speleological Society: Huntsville, AL, USA, 2000; pp. 408–426.

39. Gunn, J. *Encyclopedia of Caves and Karst Science*; Routledge: London, UK, 2004.

40. White, W.B.; Culver, D.C. *Encyclopedia of Caves*; Elsevier: Amsterdam, The Netherlands, 2005.

41. Ford, D.; Williams, P.D. *Karst Hydrogeology and Geomorphology*; John Wiley and Sons Inc.: New York, NY, USA, 2007.

42. Curl, R. Scallops and Flutes. *Trans. Cave Res. Group Great Br.* **1966**, *7*, 121–160.

43. Curl, R.L. Deducing Flow Velocity in Cave Conduits from Scallops. *Natl. Speleol. Soc. Bull.* **1974**, *36*, 22.

44. Lauritzen, S.E. Scallop Dominant Discharge. In Proceedings of the 10th International Congress of Speleology, Budapest, Hungary, 13–20 August 1989; pp. 123–124.

45. Murphy, P.J. Scallops. In *Encyclopedia of Caves*; White, W.B., Culver, D.C., Eds.; Elsevier: Amsterdam, The Netherlands, 2012; pp. 679–983.

46. Hammer, Ř.; Harper, D.A.T.; Ryan, P.D. PAST: Paleontological Statistics Software Package for Education and Data Analysis. *Palaeontoogia* **2001**, *4*, 9.

47. Woodward, E.; Sasowsky, I.D. A spreadsheet program (ScallopEx) to calculate paleovelocities from cave wall scallops. *Acta Carsologica* **2009**, *38*, 303–305. [CrossRef]

48. Palmer, A. Hydrogeologic control of cave patterns. In *Speleogenesis. Evolution of Karst Aquifers*; Klimchouk, A., Ford, D.C., Palmer, A.N., Dreybrodt, W., Eds.; National Speleological Society: Huntsville, AL, USA, 2000; pp. 77–90.

49. Lazaridis, G. Speleological research in the Loutra Arideas area (Macedonia, Greece). *Neue Forschun-Gen Zum Höhlenbären Eur.* **2005**, *45*, 57–64.

50. Lazaridis, G. Almopia Speleopark (Pella, Mac-edonia, Greece): Morphology-Speleogenesis of the caves. *Sci. Ann. Sch. Geol. Aristotle Univ. Thessalon.* **2006**, *98*, 33–40.

51. Lazaridis, G.; Melfos, V. Morphological features and formation conditions of The Almopia Speleopark caves (Loutra Almopias, N. Greece). *Acta Carsologica* **2021**, *50*, 37–48. [CrossRef]